Electric Power Systems Research 253 (2026) 112513

Contents lists available at ScienceDirect

Electric Power Systems Research

journal homepage: www.elsevier.com/locate/epsr

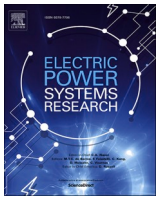

Evaluating the impact of power-frequency voltages on the indirect lightning performance of overhead distribution lines

F. Napolitano [a], M. Corti [b], F. Tossani [a,*], M. Bernardi [b], A. Borghetti [a], C.A. Nucci [a]

[a] Department of Electrical, Electronic and Information Engineering, University of Bologna, Italy
[b] Cesi S.p.A. Milano, Italy

ARTICLE INFO

Keywords:
Lightning induced overvoltages
Monte Carlo method
Overhead distribution lines
Surge arresters

ABSTRACT

This paper investigates the influence of power-frequency voltages on the indirect lightning performance of overhead distribution lines. Analyses on the subject often disregard this factor, assuming a de-energized line. However, in certain cases, e.g., when discriminating between single and multi-phases flashovers is of interest, the effect of the power-frequency voltage might be worth of investigation. The paper presents a comparative study of two methodologies implemented within the LIOV-EMTP simulation environment to account for the power-frequency voltage effects. The first method employs a rigorous approach, incorporating voltage offsets in the Bergeron lines that interconnect LIOV and EMTP. The second method, though less precise, offers a simplified approach that has the advantage of avoiding modifications to the LIOV-EMTP interface used when the line is de-energized. A statistical analysis is conducted to quantify the effect of the power-frequency voltage on the predicted number of single and multi-phase flashovers and to evaluate the effectiveness of both methods in calculating the indirect lightning performance. By considering two lines characterized by different rated voltages, a sensitivity analysis is performed for different spacing between SAs and different values of both ground conductivity and SA grounding resistance.

1. Introduction

Indirect lightnings (i.e., lightning striking the ground near the line) are a common cause of outages in medium voltage (MV) lines, as induced overvoltages can significantly exceed the normal operating voltage levels, leading to line-insulator flashovers and failures in electrical equipment. Assessing the potential threat due to such overvoltages is therefore of interest for the coordination of protections like surge arresters (SAs), which are effectively capable of reducing the risk of disruptions posed by both direct and indirect lightning events [1].

Induced overvoltages on multiconductor lines are affected by multiple factors, such as the line geometry, the lightning current waveshape, propagation and location and the ground electrical parameters. To consider the effect of induced overvoltages in distribution lines, the Lightning-Induced OverVoltage (LIOV) code [2] can be employed along with the Electromagnetic Transients Program (EMTP) (e.g [2,3]), which allows for a realistic representation of distribution-line poles, insulators and SAs.

This study is focused on assessing the effect of steady-state voltages, i.e., the conductor voltages at the power frequency (e.g., 50 Hz or 60 Hz) resulting from the line energization. The effect of the power frequency voltages has been investigated on the performance of transmission lines against direct lightning, see e.g [4], where the effect of the ac source voltage on the archorn flashover phase is shown, and [5] where the dependence of the multi-phase backflashover probability from the ac voltages is assessed but is in general not addressed in studies on indirect lightning performance of distribution lines [6–8]. The effect of the power-frequency voltages is significant for the analysis of the lightning performance in resonant-grounded distribution networks, when the distinction between flashovers occurring either on a single-phase conductor or across multiple phases simultaneously is important [9]. In the absence of power-frequency voltages, lines with conductors positioned at the same height above ground are likely to experience identical overvoltages across all insulators [7], resulting in flashovers occurring simultaneously across all phases.

Aim of this paper is first to present an analysis on the effect of the power-frequency voltages in the assessment of the lightning performance of distribution lines against indirect strokes, and second, to compare two different approaches for taking the power-frequency voltages into account. The first method employs a rigorous approach,

* Corresponding author.
E-mail address: fabio.tossani@unibo.it (F. Tossani).

https://doi.org/10.1016/j.epsr.2025.112513
Received 20 December 2024; Received in revised form 23 June 2025; Accepted 25 October 2025
Available online 25 November 2025

incorporating voltage offsets in the Bergeron lines that interconnect LIOV and EMTP, as discussed e.g., in [9–12]. The second method relies on an adjusted representation of network components within the EMTP module. This method, while less precise, offers the advantage of a simplified approach that avoids modifications to the LIOV-EMTP interface valid for de-energized lines, but in some cases provides some deviation in results in comparison with the first model. The first method was presented in [10], while the second one is an original contribution of [13], whose framework is extended in this paper by comparing the transient response of two distinct distribution line configurations. To evaluate the influence of steady-state voltages and facilitate validation of the proposed models, two configurations are selected with different nominal voltages, namely, 20 kV and 6.6 kV.

To assess whether the different predictions obtained by neglecting power-frequency voltages are statistically significant, the two models are used for estimating the lightning performance by using the Monte Carlo (MC) method illustrated in [8]. A sensitivity analysis is performed to assess the impact of different spacing between SAs, as well as different values of the ground conductivity and SA grounding resistance.

The paper is structured as follows. Section II presents the two models adopted for taking the steady-state voltage into account. Section III describes the LIOV-EMTP models of the two considered line configurations and the Monte Carlo procedure. Section IV presents the results by assessing the impact of mains-frequency voltage in different case studies. Section V concludes the paper.

2. Steady-State voltage representation in LIOV

The LIOV code [2] calculates the lightning-induced overvoltages on multi-conductor overhead lines by using an engineering return stroke model of the distribution of the current along a vertical lightning channel, as shown by the geometry of the problem illustrated in [14,15] and [12]. Different engineering return stroke models can be used in the LIOV code. In this paper, the Master and Uman TL model [16] is used, in order to take advantage of the reduced computational cost enabled by the analytical approach presented in [17] for the electromagnetic field computation. The LIOV code solves the equations of the electromagnetic field described in [18] by using a one-dimensional Finite-Difference Time-Domain (FDTD) technique. The spatial step is taken at the limit of the Courant stability criterion. The results presented in this paper are obtained by adopting spatial and time steps equal to 5 m and 16.67 ns, respectively.

To extend its applicability to realistic power systems, LIOV is integrated with the EMTP (e.g [2,3]), enabling the simulation of distribution networks incorporating diverse components such as transformers, SAs, and by considering flashover occurrence in the simulation too. The interface between LIOV and EMTP is achieved through the application of Bergeron's method. The input data for the LIOV-EMTP code specify the topology of the overhead lines illuminated by the electromagnetic field generated by the lightning, the geometrical data of the poles of the overhead line for the calculation of the per-unit-length parameters, the lightning stroke position with respect to the line, the engineering return stroke model and the lightning waveform at the base of the channel. The code uses the Cooray-Rubinstein formula [19,20] to account for the effect of the ground conductivity and permettivity on the horizontal component of the electric field. Additional information on the input data of the LIOV-EMTP code, together with application examples, con be found in [12].

Instead of explicitly modeling the sinusoidal waveform, the power-frequency voltages are treated as constant DC offsets. This approximation is justified by the fact that the period of the power frequency voltage is 16.7 or 20 milliseconds, substantially longer than the microsecond timescale of the induced overvoltages, making the sinusoidal variation negligible during the transient event.

Within the LIOV-EMTP interface, two distinct approaches are utilized for incorporating these steady-state voltage offsets. A rigorous method directly integrates the power-frequency voltage representation in the Bergeron line model used for the LIOV-EMTP coupling. This approach ensures a higher degree of accuracy in representing the interaction between the steady-state and transient phenomena. Alternatively, a simplified technique, termed the "method of the dc voltage offset" involves modifying specific network components within the EMTP environment to effectively introduce the required dc offset. This simplified approach offers computational efficiency while still providing a reasonable approximation of the power-frequency voltage influence on the transient response.

2.1. Method of the modified Bergeron equivalent generators

The interface between LIOV and EMTP is achieved through a discretized representation of the line, employing a series of short sections. In the LIOV-EMTP module presented in [3], for each line section the field-to-line coupling equations are solved by implementing a FDTD scheme. Fig. 1 depicts the single-conductor equivalent circuit which is based on the application of Bergeron's method.

The generators of the equivalent circuits seen by EMTP, i.e. G_1 and $G_{\mathrm{kmax}-1}$ in Fig. 1, are set equal to the backward and forward voltage waves, respectively. According to [3], a term is also added to account for the effect of the external horizontal electric field. Moreover, a term V has to be added to account for the steady state voltage, as shown below

$$G_1 = v_1^n - Ev_0^{n+1}h - Zi_1^n - \frac{\Delta x}{2}\left(Eh_0^{n+1} + Eh_1^n\right) + V \tag{1}$$

$$G_{\mathrm{kmax}-1} = v_{\mathrm{kmax}-1}^n - Ev_{\mathrm{kmax}}^{n+1} + Zi_{k_{\mathrm{max}}-1}^n + \frac{\Delta x}{2}\left(Eh_{k_{\mathrm{max}}}^{n+1} + Eh_{k_{\mathrm{max}}-1}^n\right) + V \tag{2}$$

where, for spatial index k and temporal index n:

- v_k^n, i_k^n are the scattered voltage and the current along the line;
- Ev_k^n, Eh_k^n are the components of the external field in vertical direction and along the line;
- Δx is the spatial step of FDTD scheme and the length of the Bergeron lines;
- Z and V are the surge impedance and the steady state voltage of the line, respectively.

Further details, e.g. the treatment of line ends terminated with the surge impedance matrix, are described in [11,12]. This method will herafter also be referred to more simply as method *A*.

2.2. Method of the dc voltage offset

This method assumes a standard interface between LIOV and EMTP, i.e. Eqs. (1) and (2) without the addition of the steady-state voltage V. The method consists in adding an ideal dc voltage source in series to the SAs with amplitude equal to the steady-state value of the phase to ground voltage, while keeping the line not energized. The voltage generators directed from the line towards the arrester, so as to subtract from the incident voltages on the SA the power-frequency voltage value.

When present, the flashover model is subject to corresponding adjustments too. In this study, the integration model [21] is employed to simulate insulator flashovers. This particular model is regarded as more realistic, as it accounts for both the amplitude of the peak voltage and the characteristics of the overvoltage waveform in determining the occurrence of flashover events. The model's foundation is built upon the following integral formulation

$$D = \int_{t_0}^{t} \left(|v(t)| - V_0\right)^k dt \tag{3}$$

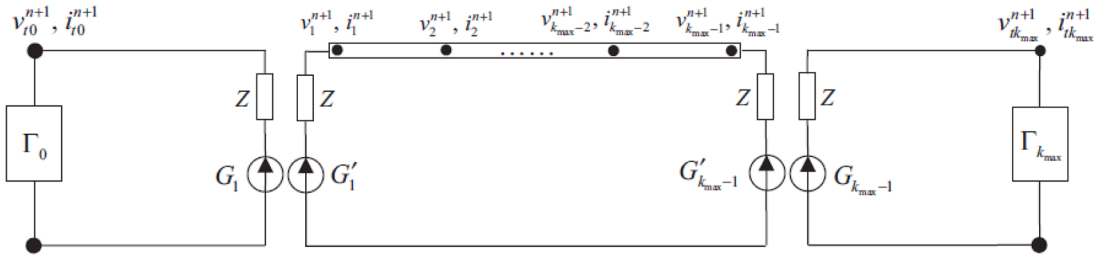

Fig. 1. Equivalent circuits for the interface between LIOV and EMTP.

in which: $v(t)$ represents the voltage across the pole insulator; V_0 is the minimum voltage necessary for triggering any breakdown process; k is a dimensionless factor; t_0 is the time instant when the magnitude of $|v(t)|$ first exceeds V_0. In case integral D becomes larger than a certain value DE, a flashover is counted.

The method of the steady-state voltage effect requires the modification of the flashover model by subtracting the steady-state voltage from V_0. This method will herafter also be referred to more simply as method B.

3. Description of the LIOV models and of the calculation procedure

Fig. 2 illustrates the pole geometries for the two considered line configurations: a 20-kV line (left) and a 6.6-kV line (right). Both configurations feature a vertical pole supporting a horizontal cross-arm equipped with three insulators for conductor placement. The 20-kV line configuration has a shorter pole and a wider spacing between the insulators with respect to the 6.6-kV line configuration, which is characterized by a taller pole and narrower insulator spacing. The main structural and electrical parameters of the two considered line configurations are summarized in Table 1: the characteristics of the conductors, including their height, diameter, and spatial arrangement, as well as the insulator models and pole surge impedance.

The flashover models for a 25-kV pin-type and a 6.6-kV solid-core-type insulator have been derived utilizing the voltage-time characteristics obtained from dielectric strength tests reported in [22] and [23], respectively. The methodology employed to determine the parameters of the integration-based model is detailed in [23]. Based on this approach, the extracted parameters for the insulator are: V_0= 124.8 kV and DE = 86.7 kVμs for the 20-kV line insulators and V_0= 132 kV and DE = 66 kVμs for the 6.6-kV one. The model of the surge arresters adopted in the two configurations are the ones described in [13] and [23], for the two configurations respectively.

Table 1
Main structural and electrical parameters of the two considered line configurations.

	Line configuration	
	20 kV [13]	6.6 kV [24]
Conductors height	10 m	11.375 m
Conductors diameter	1 cm	1.16 cm
Positions of conductors	$x_1 = -1$ m, $x_2 = 0$ m, $x_3 = 1$ m	$x_1 = -0.5$ m, $x_2 = 0.5$ m, $x_3 = 1$ m
Insulator model	$V_0 = 124.8$ kV, $DE = 86.7$ kVμs	$V_0 = 132$ kV, $DE = 66$ kVμs
Pole surge impedance	$Z_s = 300\ \Omega$	$Z_s = 300\ \Omega$
SA model	Dynamic [13]	Static [23,24]
SA residual voltage at 1 kA	80 kV (for a 8/20 μs waveform)	25 kV

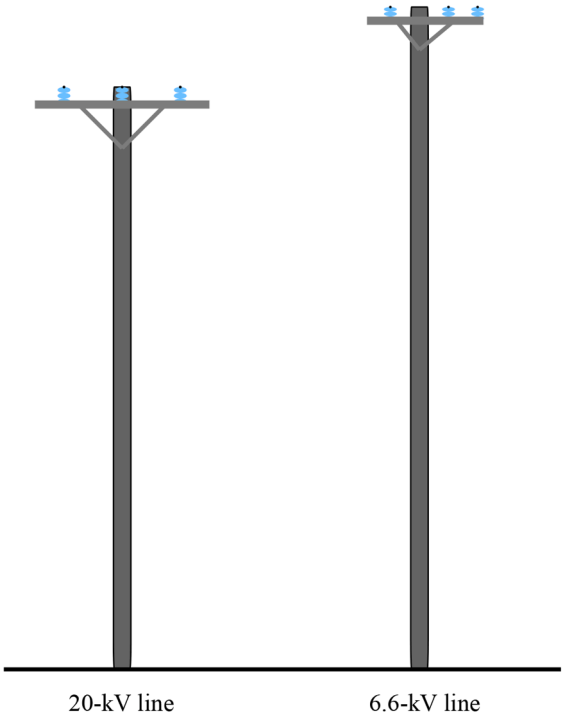

Fig. 2. Pole geometry of the two considered line configurations.

3.1. Description of the Monte Carlo procedure

The waveform of induced overvoltages is affected by the characteristics of the channel-base current. In the context of lightning performance assessments for distribution lines using MC simulations, it is a common practice to model the channel-base current as a ramp followed by a flat top [1]. However, in this study, the overvoltages are computed using Cigré functions [25], which provide a more accurate representation of the realistic return-stroke current waveforms. The Cigré current model is defined by four parameters: peak amplitude I_p, front time t_f, maximum front steepness S_m and wave-tail time to half value t_h. Notably, these parameters exhibit interdependence, requiring a multivariate distribution approach for their generation. A specific procedure is therefore employed to generate MC events, ensuring the correlated nature of the lightning current parameters, as detailed in [26]. Only first negative return strokes are considered in this paper, following the typical assumptions made in the statistical assessment of lightning performance calculations. It is worth noting that subsequent strokes with larger peak than first ones may occur and can be threatening due to their typical increased steepness [27]. The effect of the subsequent strokes could be more or less evident according to the network configuration and flashover model as analyzed in [28,29].

The spatial distribution of the lightning events is uniformly randomized, with x and y coordinates spanning a 1-km distance from the line, which itself extends 2 km in length and is matched at both terminations. Direct and indirect lightning events are classified using the electro-geometric model [1]. The considered ground conductivity σ_g is 1

mS/m, if not otherwise specified. The distance of 1 km from the line is enough to account for all the indirect events able to induce overvoltages with amplitude larger than the minimum considered CFO and the minimum SA discharge current. This distance is influenced by the presence of SA installed along the line, as in the considered case. Further indications on the choice of the minimum distance from the line are provided in [30]. The Transmission Line (TL) model is employed to represent the return stroke, with velocity equal to 1.5×10^8 m/s, representative of the speed of lowest portion of the lightning channel [31], which has a major influence on lightning induced overvoltage amplitudes [32]. For each of the MC events, the power-frequency voltage values of the three phase conductors are randomly chosen, by assuming they form a positive sequence and follow a uniform probability distribution.

The statistical procedure based on the MC method is implemented in a Matlab environment which repeatedly calls LIOV-EMTP simulations by modifying the EMTP settings before each run and collecting the relevant results after each execution.

4. Impact of power frequency voltage in LIOV calculations

4.1. Influence on the multiplicity and location of flashovers

In this Subsection, the results relevant to the time-domain analysis of the considered distribution lines is presented, with focus on the impact of the mains-frequency voltage on the expected number of multi-phase flashovers.

The line is matched at both terminations, and SAs are placed at 500-meter intervals. The SAs are grounded with resistance $R_g = 20\ \Omega$. Two different stroke locations are considered, both at a distance of 70 m from the line, as depicted in Fig. 3. The channel-base current – the same for both the considered stroke locations – was selected from a broader set of simulated indirect lightning events generated through the MC procedure and is characterized by the following parameters: $I_p = 47$ kA, $t_f = 4.6$ μs and $S_m = 38$ kA/μs.

Fig. 4 shows the peak overvoltage amplitudes along the line caused by an indirect lightning stroke occurring at $x = 1250$ m, $y = 70$ m (stroke location 2). The time-domain overvoltages across pole 25, which is located at $x = 1250$ m, and 26 are reported too. For the considered line geometry the induced voltages have the same magnitude in all phases [33], as confirmed by the time-domain overvoltages across pole 25 and 26 insulators. Such overvoltages, calculated by neglecting the steady-state power-frequency voltage, induce simultaneous flashovers on all three phases at the poles nearest the stroke location (poles 24, 25, and 26, as indicated by red marks).

In case the same event is reproduced by taking into account the steady-state voltages (Fig. 5), a flashover occurs in phase-1 insulator at pole 25 and in phase 2 at poles 24 and 26. The reason for the observed differences is the following: although for the considered line geometry the induced voltages have the same magnitude in all phases, including the power-frequency voltages result in a different total voltage across the three-insulators. When one phase flashes over at a pole, it effectively reduces the potential difference across the other phases at that same pole, preventing them from flashing over too. For instance, a flashover in phase 1 at pole 25 prevents flashovers in phases 2 and 3 at that pole. Likewise, a flashover in phase 2 at pole 26 prevents flashovers in phases 1 and 3.

4.2. Comparison between the two methods

This Subsection compares the time-domain waveform of the SAs voltages and currents obtained by the two calculation methods described in Section 2. The same channel-base current with 47-kA peak is considered, but the simulations result are relevant to stroke location 1, which is in front of a pole equipped with SAs.

Fig. 6 compares SAs voltage and current waveforms obtained by using the two calculation methods. Although the voltage across the three SAs calculated by using method *A* differ significantly from the total voltages across the series-connected DC voltage source and SAs obtained by method *B*, both methods predict nearly identical discharge currents.

The comparison for the 6.6-kV configurations (Fig. 7) yields to the same considerations, indicating that method *B* predicts similar SAs discharge currents as the more accurate method *A* irrespective of the SAs rated voltage.

4.3. Statistical analysis for the 20-kV line

The annual number of flashovers per 100 km of line is calculated as:

$$F_p = 200 \frac{n}{n_{tot}} y_{\max} N_g \tag{4}$$

where n is the number of events causing insulator flashovers, $n_{tot} = 20{,}000$ is the number of events considered in the MC procedure, $y_{\max} = 1$ km is the maximum value of the distribution of stroke position coordinate y, and N_g is the ground flash density, assumed equal 1 flash/km^2/year.

The annual number of events causing a flashover in at least one

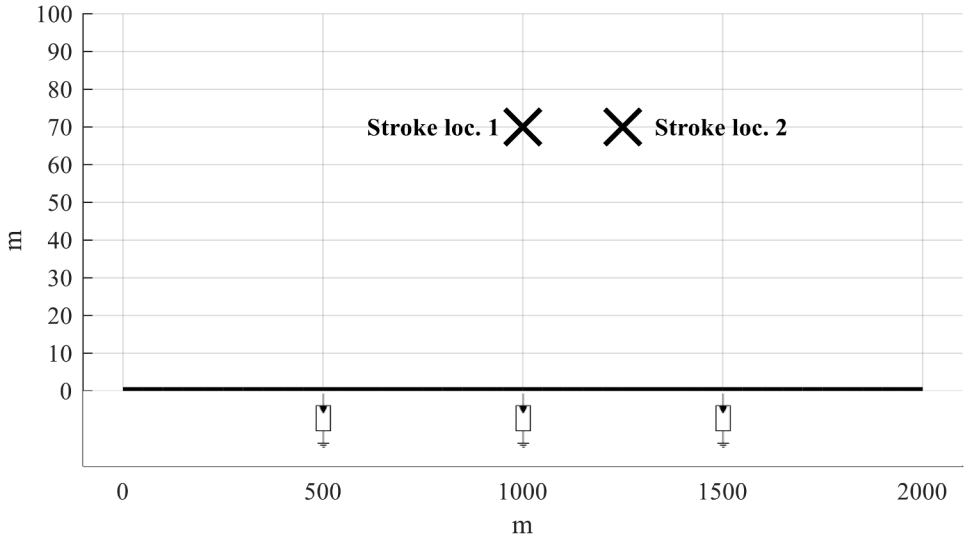

Fig. 3. Line topology and stroke locations. SAs are installed every 500 m.

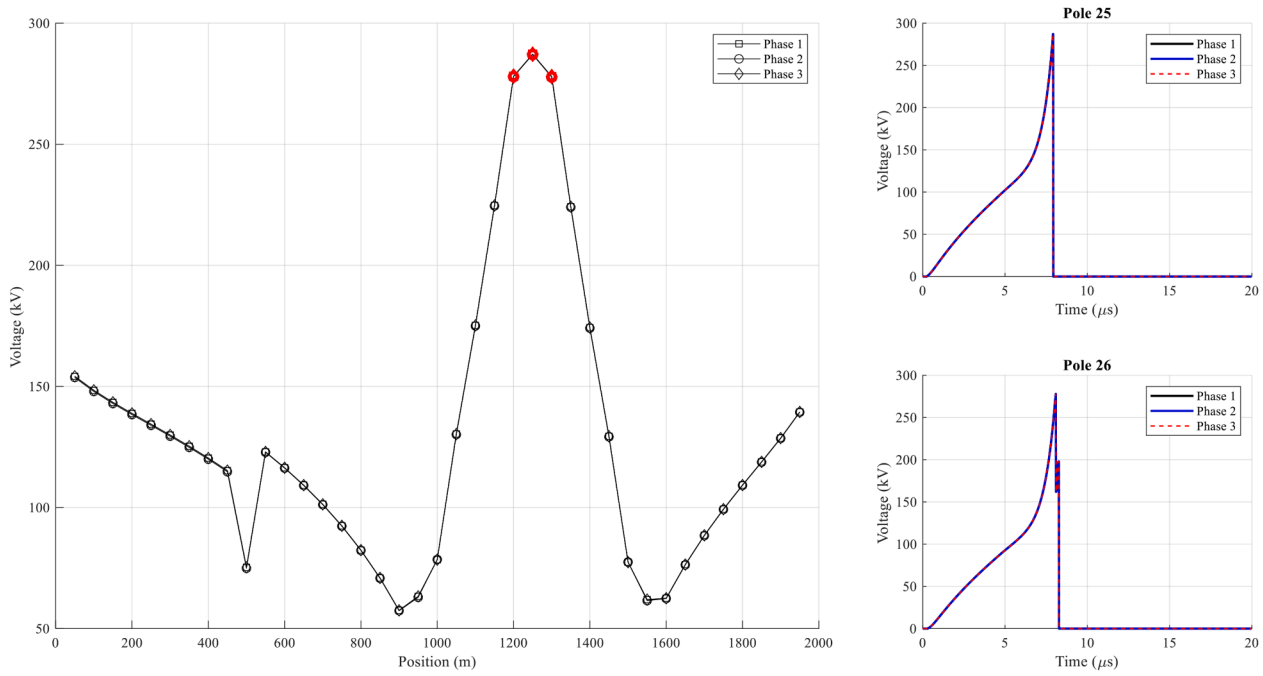

Fig. 4. Voltage (peak amplitudes on the left and time domain on the right) across insulators neglecting the steady-state voltages. All phases are affected by a flashover in three different poles: 24, 25 and 26 (red marks indicate flashovers). Stroke location 2.

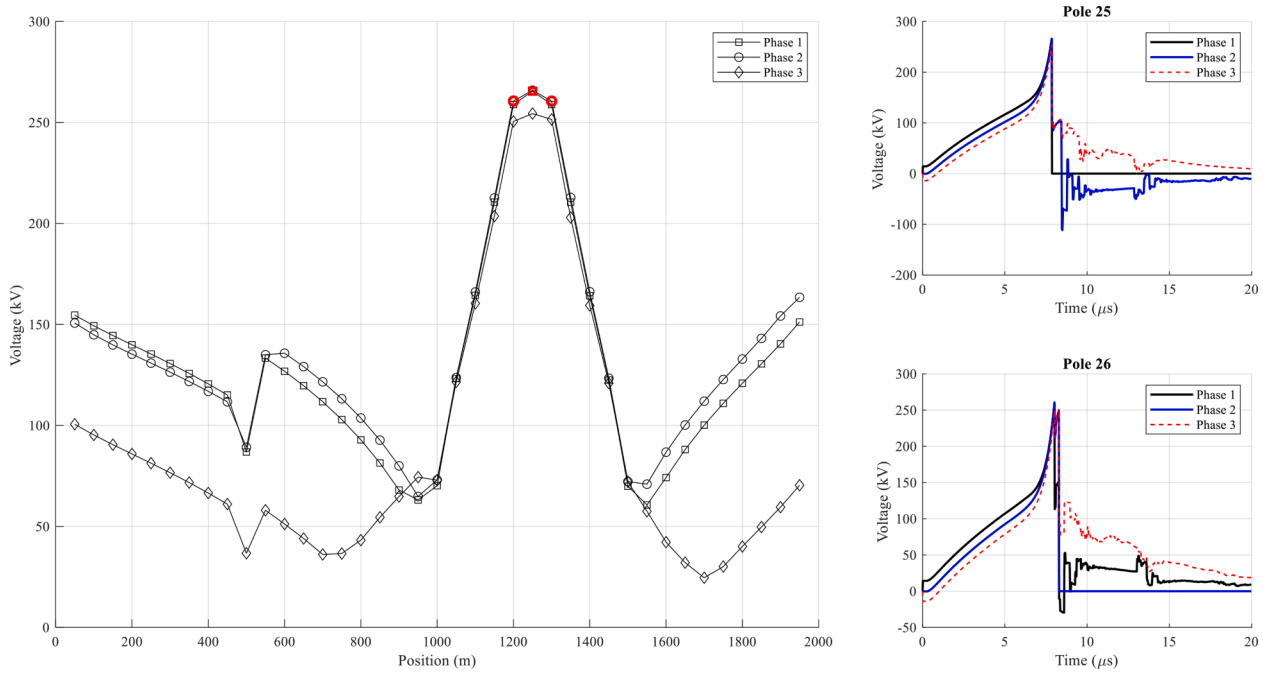

Fig. 5. Voltage (peak amplitudes on the left and time domain on the right) considering the steady-state voltages by using method A. Single-phase flashovers occur in phase-1 insulator at pole 25 and in phase 2 at poles 24 and 26 (red marks indicate flashovers). Stroke location 2.

phase-insulator is reported in Fig. 8 along with the number of events originating flashovers in multiple phase-insulators simultaneously. The figure confirms that neglecting the steady-state voltages can lead to overestimate the number of multi-phase flashovers and, conversely, to underestimate the total number of events resulting in a flashover. The approximated method tends to overestimate the total number of flashovers while underestimating the occurrence of multiple phase flashovers compared to Method *A*. Notably, when the ground conductivity is increased to 10 mS/m, the two methods yield the same results. On the other hand, with a ground conductivity σ_g of 10 mS/m, the induced voltage peaks are significantly reduced, diminishing their relative importance compared to steady-state voltages. In such circumstances, neglecting the power-frequency voltage can lead to an underestimation of the total number of flashovers and an overestimation of multi-phase flashover occurrences.

The differences between the results predicted by the two methods appear to be more meaningful if the spacing between subsequent SAs is reduced to 200 m, as shown in Fig. 9. In this scenario, method *B*

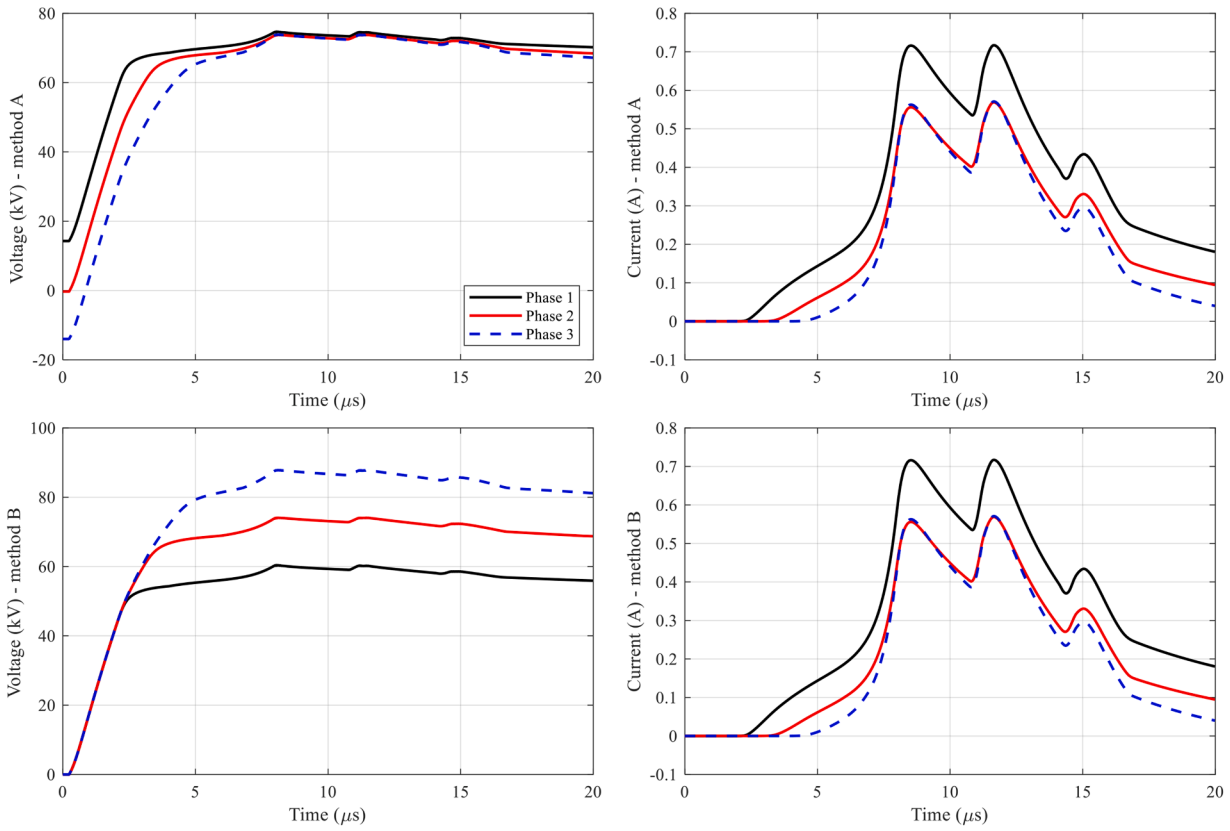

Fig. 6. Voltage and discharge currents of SAs for the two considered methods. 20 kV config., stroke location 1.

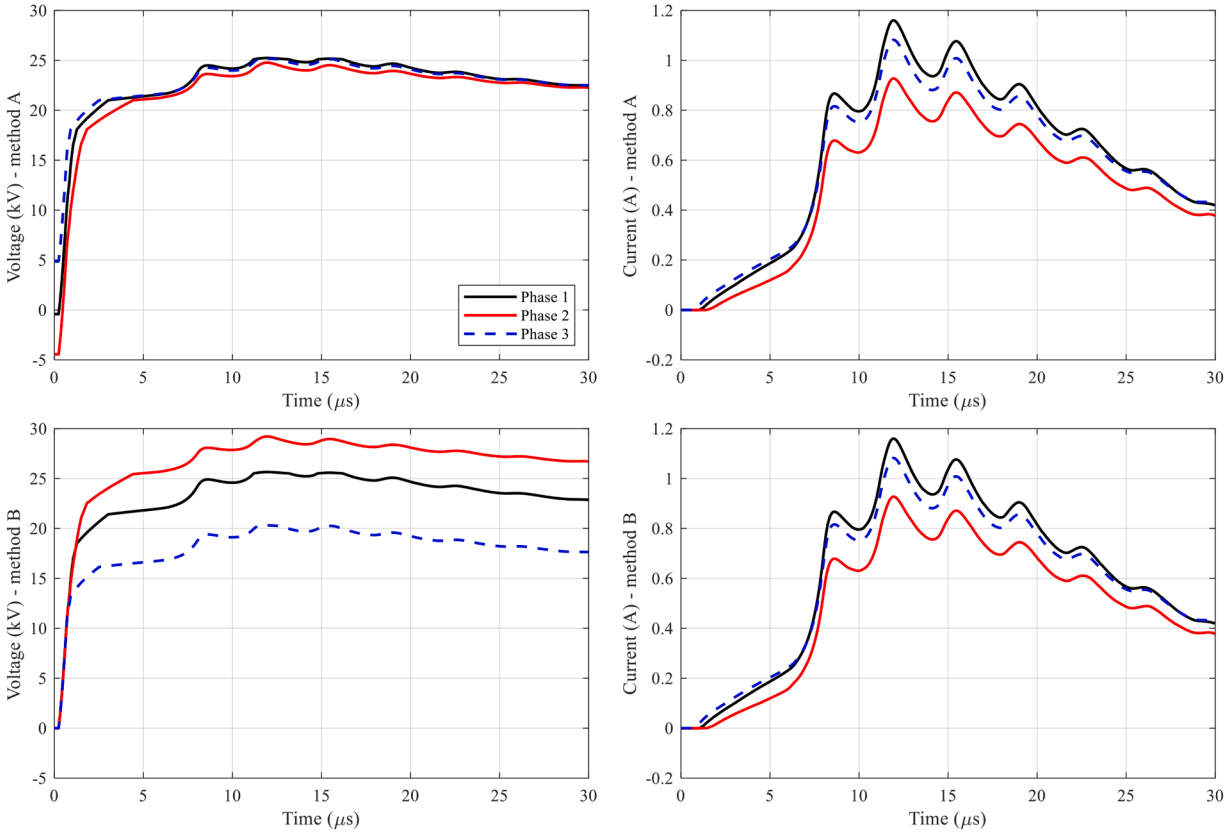

Fig. 7. Voltage and discharge currents of SAs for the two considered methods. 6.6 kV config., stroke location 1.

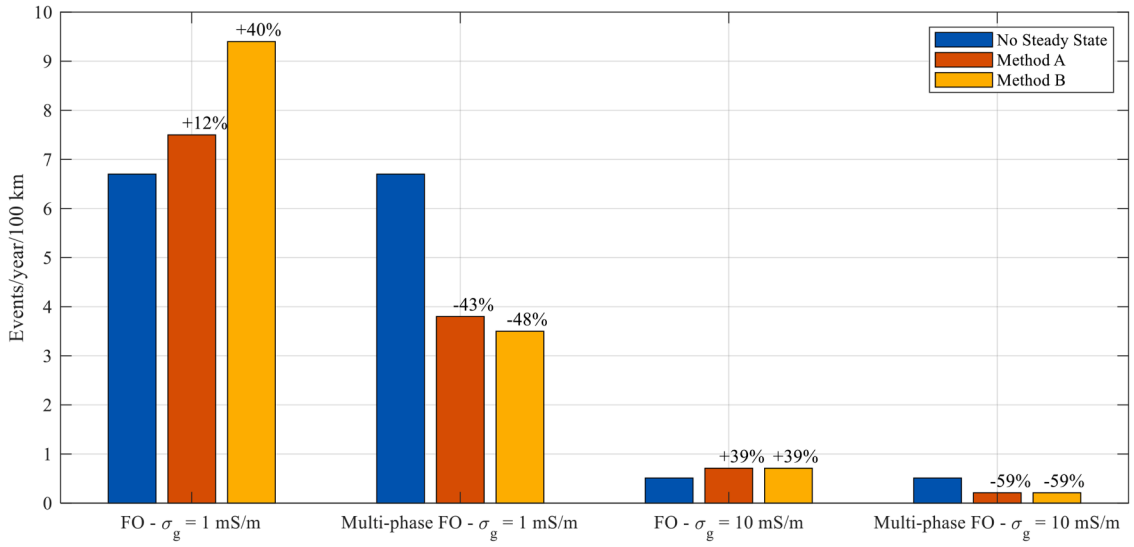

Fig. 8. Annual number of flashovers (FO) per 100 km for different ground conductivity values. 20 kV configuration, SAs spacing = 500 m.

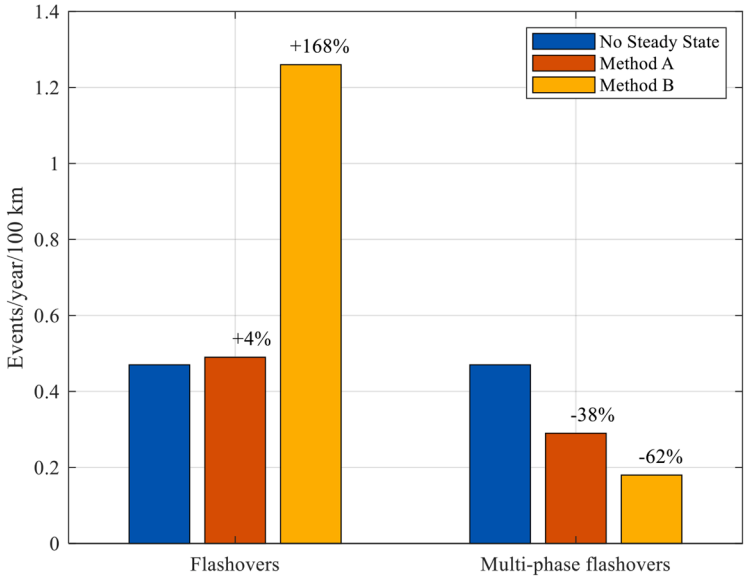

Fig. 9. Annual number of flashovers/100 km for the 20-kV configuration. SAs spacing = 200 m.

overestimates the number of flashovers by more than 150 %.

Fig. 10 compares the results obtained by the different calculation methods when assessing the rate of indirect events able to induce currents larger than the value in abscissa in at least one of the SAs. Fig. 10 considers an SA spacing of 500 m, while Fig. 11 refers to the case of 200 m spacing. In both cases, the omission of steady-state voltages leads to an underestimation of current peaks. The methods show good agreement for currents below 600 A; indeed, when the higher ground conductivity value is considered, both methods yield the same value of SAs current. Instead, for the case with $\sigma_g = 1$ mS/m, method *B* tends to overestimate the annual rate predicted by method *A* for larger current values, particularly at the wider SA spacing of 500 m.

Fig. 12 presents a comparison of the two methods under the assumption that flashovers are disregarded. In this scenario, the outcomes align closely, indicating that the discrepancies observed in Fig. 10 and Fig. 11 can be attributed to the surges induced by flashovers occurring along the line.

Fig. 13 illustrates the flashover rate derived from the two methods, represented as the annual number of events per unit length that generate overvoltage peaks exceeding 1.5 times the line critical flashover voltage (CFO) [1]. This analysis reaffirms the consistency between the two approaches when the effects of insulation breakdown are excluded from the calculations.

4.4. *Influence of the SAs grounding resistance*

The effect of increasing a the SAs grounding resistance is to worsen the lightning performance of the line [34]. Fig. 14 shows the expected annual number of flashovers in case SAs grounding resistance R_g is increased to 50 Ω. Under these assumptions, the peak value of the current flowing in the SAs diminishes, therefore, the differences between the two methods are lower than in Fig. 8.

4.5. *Comparison with the 6.6-kV line*

Fig. 15 presents the expected flashover rates for the 6.6-kV configuration. This second configuration shows a better performance respect to the 20-kV one, mainly due to the significantly lower residual voltage

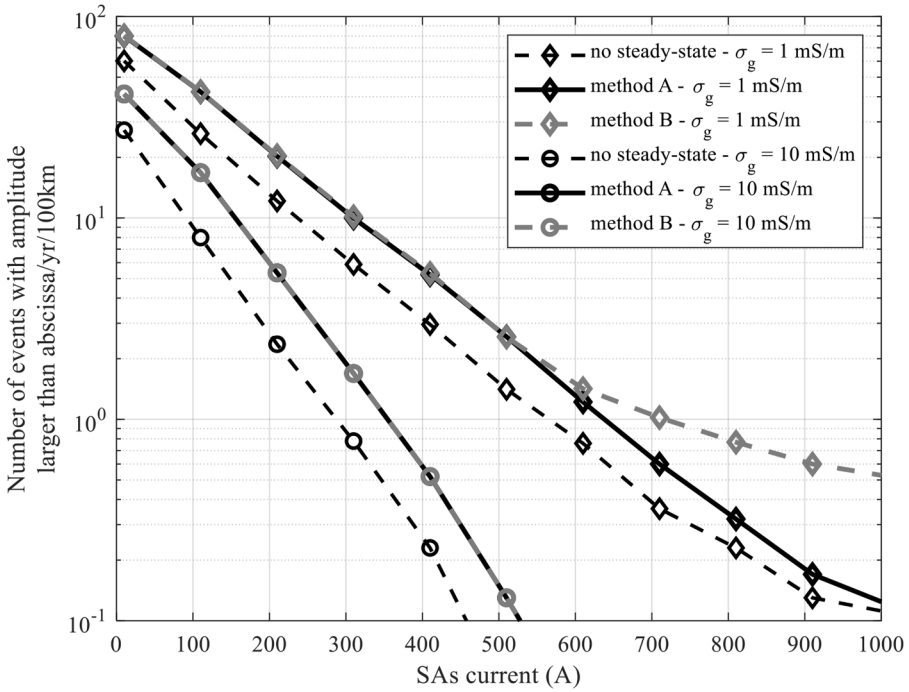

Fig. 10. Number of events with currents exceeding the value in abscissa in at least one of the SAs per year per 100 km. Comparison between different calculation methods and ground conductivities. Distance between SAs = 500 m.

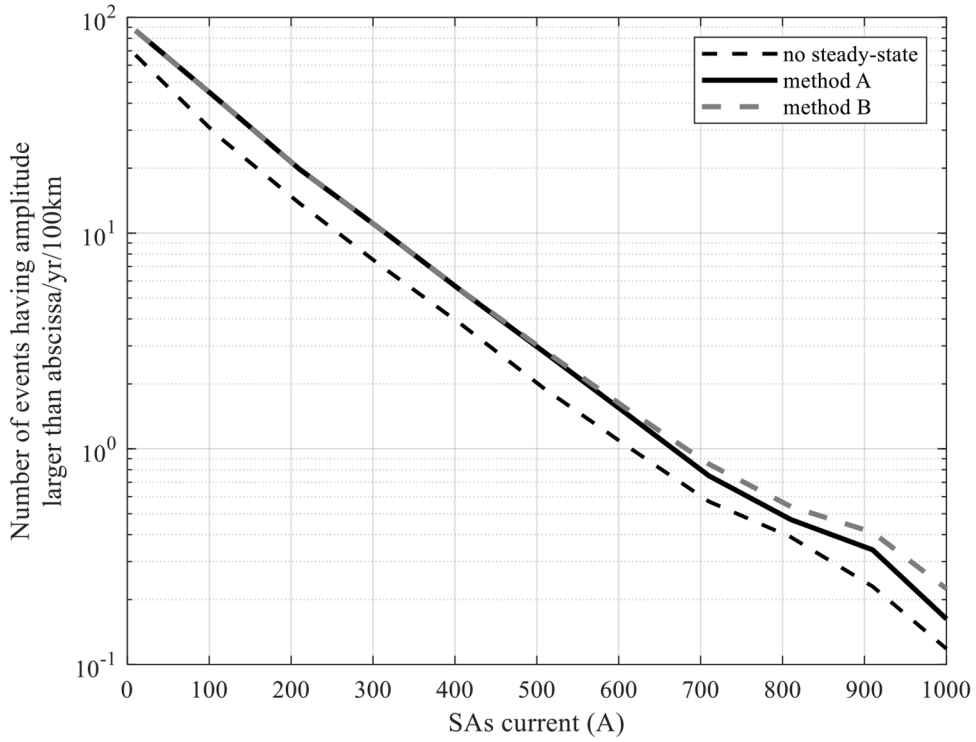

Fig. 11. Number of events with currents exceeding the value in abscissa in at least one of the SAs per year per 100 km. Comparison between different calculation methods. Distance between SAs = 200 m.

of the adopted SAs (see [23] and [13]).

Comparing these results with those in Fig. 8 reveals lower discrepancies between method B and the more accurate method *A*. This can be attributed to the lower rated voltage of the 6.6-kV line compared to the previous configuration, which diminishes the relative influence of the power-frequency voltages on the total voltage across insulators.

Typically, this 6.6-kV line configuration has a shield-wire on top of the pole [23] to improve the line performance against direct strikes. Such line configurations, equipped with both shied-wire and SAs, are therefore extremely well protected against indirect strokes. Simulations were also conducted with the inclusion of the shield wire, confirming that as the level of protection increases – resulting in reduced current

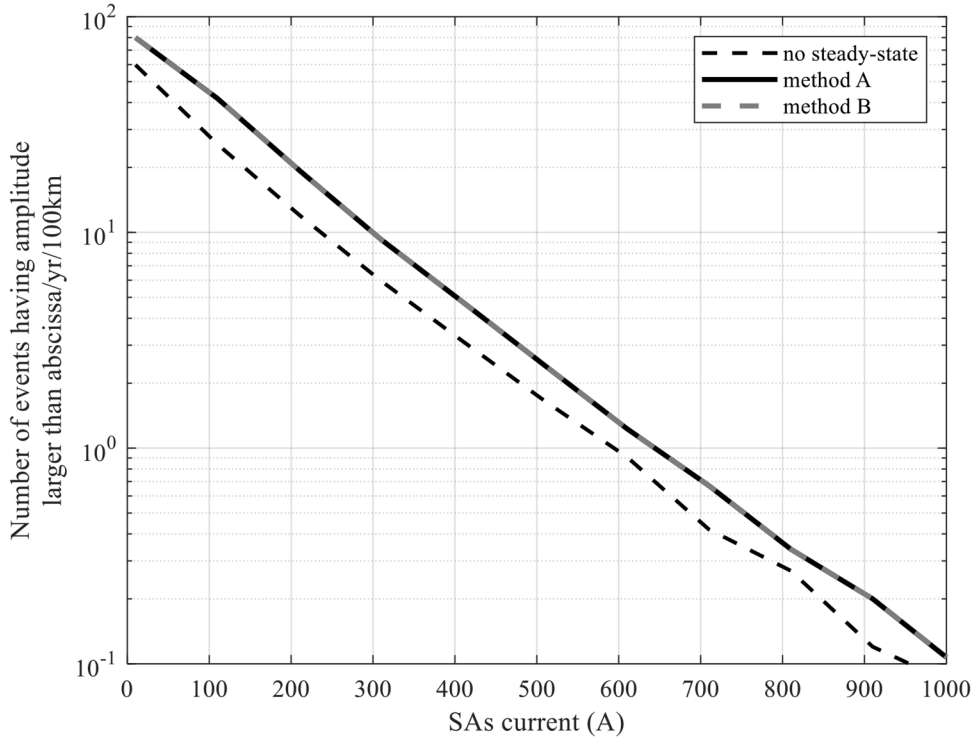

Fig. 12. Number of events with currents exceeding the value in abscissa in at least one of the SAs per year per 100 km. Flashover occurrence is neglected. Distance between SAs = 500 m.

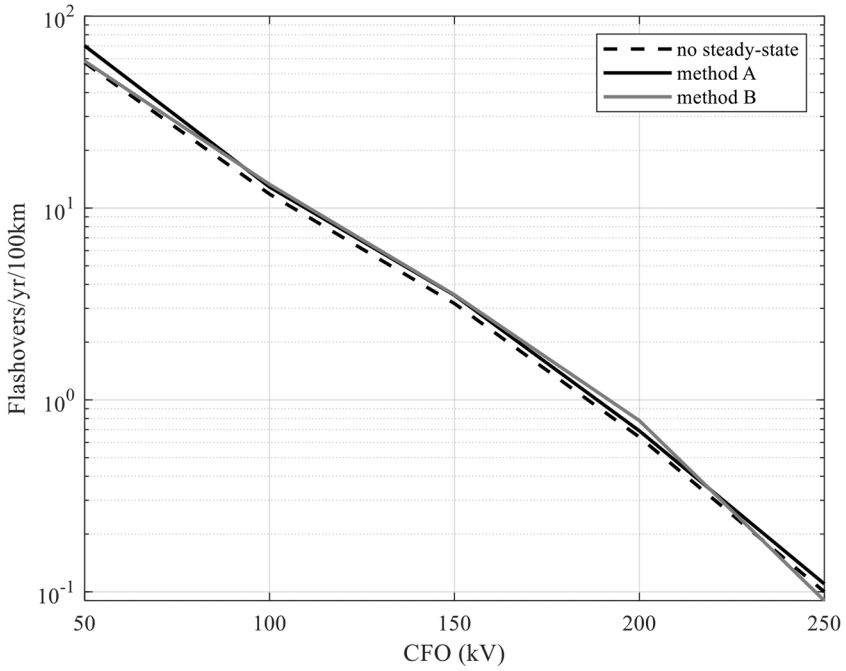

Fig. 13. Annual number of flashovers calculated as in [1]. SAs spacing = 500 m.

drained by SAs – the differences between the two methods become increasingly negligible.

5. Conclusions

The effect of the power-frequency voltage is typically disregarded in the calculation of the response to indirect lightning of distribution lines. Therefore, indirect lightning performance is often assessed as if the network were unenergized. The power-frequency voltage is known to have a non-negligible effect when the occurrence of flashovers involving more than one phase is of interest, e.g. in medium voltage with resonant grounded neutral. The paper presents and compares two approaches to account for the power frequency voltage. The first makes use of a modification of the Bergeron equivalent generators used to interface LIOV and EMPT, the other approach uses additional voltage DC sources in series to the surge arresters and the same version of LIOV-EMTP used

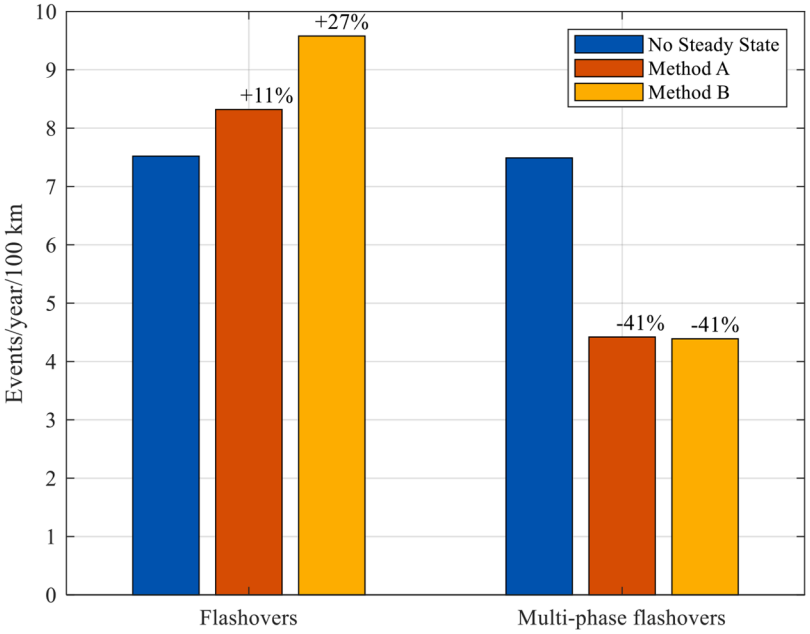

Fig. 14. Annual number of flashovers/100 km for the 6.6-kV configuration. SAs spacing = 500 m. R_g = 50 Ω.

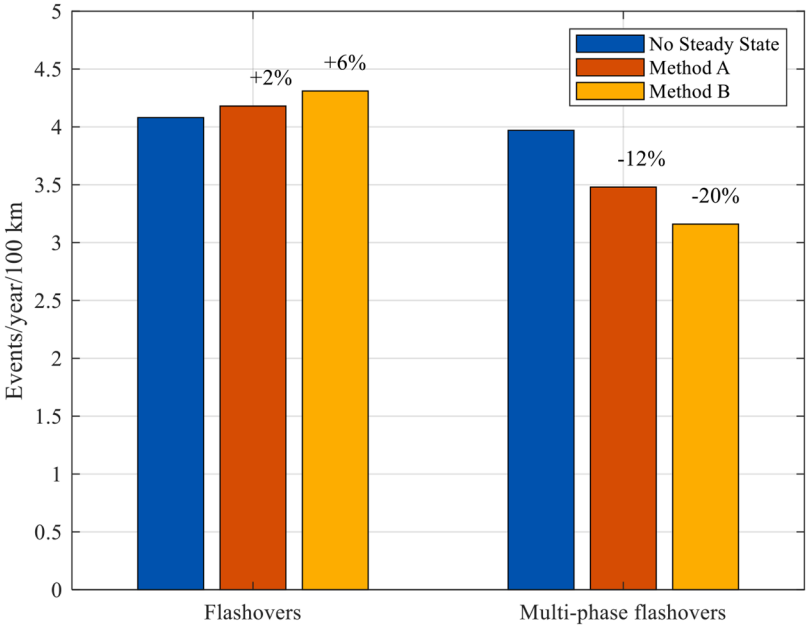

Fig. 15. Annual number of flashovers/100 km for the 6.6-kV configuration. SAs spacing = 500 m.

for de-energized lines. The adequacy of the two approaches is assessed and compared by considering two different medium voltage line topologies, rated 20 kV and 6.6 kV, different spacings among surge arresters, different ground conductivities ad grounding resistances. A statistical approach is used for the calculation of the incidence per year of the amplitudes of discharge currents in the surge arresters as well as the number of single and multiple flashovers, which are inferred by using a flashover model based on the integration method. The two approaches provide nearly identical results, with some significant deviation only where indirect lightning stress is more severe, particularly for the line at higher rated voltage, in which the effect of the utility frequency is larger, for the case of more distant surge arresters and/or the lowest values of grounding conductivity. In case of grounding conductivity of 10 mS/m the two approaches are assessed to be both valid, while with conductivity of 1 mS/m the modified Bergeron equivalent generators approach appears more accurate. Both approaches estimate a greater number of flashovers, when compared with the calculations performed neglecting the utility frequency voltage, but fewer multiple single-phase to ground faults.

CRediT authorship contribution statement

F. Napolitano: Writing – review & editing, Writing – original draft, Validation, Software, Methodology, Conceptualization. **M. Corti:** Writing – review & editing, Writing – original draft, Methodology, Conceptualization, Validation, Supervision. **F. Tossani:** Writing – review & editing, Writing – original draft, Software, Methodology, Conceptualization. **M. Bernardi:** Writing – review & editing, Writing –

original draft, Methodology, Conceptualization. **A. Borghetti:** Writing – review & editing, Writing – original draft, Validation, Supervision, Methodology, Conceptualization. **C.A. Nucci:** Writing – review & editing, Writing – original draft, Supervision, Methodology, Conceptualization.

Declaration of competing interest

The authors declare that they have no known competing financial interests or personal relationships that could have appeared to influence the work reported in this paper.

Data availability

Data will be made available on request.

References

[1] IEEE guide for improving the lightning performance of electric power overhead distribution lines, IEEE Std. (2011) 1410–2010.

[2] C.A. Nucci, F. Rachidi, Interaction of electromagnetic fields generated by lightning with overhead electrical networks, Light. Flash. (2014) 559–609, https://doi.org/10.1049/PBPO069E_ch12.

[3] F. Napolitano, A. Borghetti, C.A. Nucci, M. Paolone, F. Rachidi, J. Mahseredjian, An advanced interface between the LIOV code and the EMTP-RV, in: 29th Int. Conf. Light. Prot, Uppsala, Sweden, 2008.

[4] A. Ametani, T. Kawamura, A method of a lightning surge analysis recommended in Japan using EMTP, IEEE Trans. Power Deliv. 20 (2005) 867–875, https://doi.org/10.1109/TPWRD.2004.839183.

[5] A. Yamanaka, N. Nagaoka, Y. Baba, Lightning surge analysis of HV transmission line: bias AC-voltage effect on multiphase back-flashover, IEEE Trans. Power Deliv. 36 (2021) 3570–3579, https://doi.org/10.1109/TPWRD.2020.3045170.

[6] A. Piantini, J.M. Janiszewski, The use of shield wires for reducing induced voltages from lightning electromagnetic fields, Electr. Power Syst. Res. 94 (2013) 46–53, https://doi.org/10.1016/j.epsr.2012.04.012.

[7] J.O.S. Paulino, C.F. Barbosa, I.J.S. Lopes, W.Do Couto Boaventura, G.C. De Miranda, Indirect lightning performance of aerial distribution lines considering the induced-voltage waveform, IEEE Trans. Electromagn. Compat. 57 (2015) 1123–1131, https://doi.org/10.1109/TEMC.2015.2421315.

[8] A. Borghetti, C.A. Nucci, M. Paolone, An improved procedure for the assessment of overhead line indirect lightning performance and its comparison with the IEEE Std . 1410 method, IEEE Trans. Power Deliv. 22 (2007) 684–692.

[9] F. Napolitano, A. Borghetti, C.A. Nucci, M.L.B. Martinez, G.P. Lopes, G.J.G. Dos Santos, Protection against lightning overvoltages in resonant grounded power distribution networks, Electr. Power Syst. Res. 113 (2014) 121–128, https://doi.org/10.1016/j.epsr.2014.02.022.

[10] A. Borghetti, F. Napolitano, C.A. Nucci, M.L.B. Martinez, G.P. Lopes, J.I.L. Uchoa, Protection systems against lightning-originated overvoltages in resonant grounded power distribution systems, in: 2012 Int. Conf. Light. Prot, IEEE, Vienna, Austria, 2012, https://doi.org/10.1109/ICLP.2012.6344411.

[11] A. Borghetti, F. Napolitano, C.A. Nucci, F. Rachidi, M. Rubinstein , Telegrapher...s equations for field-to-transmission line interaction , in: F. Milano (Ed.) , Adv. Power Syst. Model. Control Stab. Anal. , 2nd ed. , 2022 , pp. 3 –44 , https://doi.org/10.1049/pbpo217e_ch1.

[12] A. Borghetti, W.A. Chisholm, F. Napolitano, C.A. Nucci, F. Rachidi, F. Tossani , Software tools for the lightning performance assessment , in: A. Piantini (Ed.) , Light. Interact. with Power Syst. , 2020 , pp. 425 –452 , https://doi.org/10.1049/PBPO172G_ch12.

[13] F. Napolitano, M. Corti, F. Tossani, M. Bernardi, A. Borghetti, C.A. Nucci, Impact of mains-frequency voltage on lightning induced overvoltages in surge protected lines, in: 17th Int. Symp. Light. Prot. SIPDA 2023, 2023, https://doi.org/10.1109/SIPDA59763.2023.10349100.

[14] C.A. Nucci, F. Rachidi, M.V. Michel, C. Mazzetti, Lightning-induced voltages on overhead lines, IEEE Trans. Electromagn. Compat. 35 (1993) 75–86, https://doi.org/10.1109/15.249398.

[15] F. Rachidi, C.A. Nucci, M. Ianoz, C. Mazzetti, Response of multiconductor power lines to nearby lightning return stroke electromagnetic fields, IEEE Trans. Power Deliv. 12 (1997) 1404–1411, https://doi.org/10.1109/61.637022.

[16] M.J. Master, M.A. Uman, Transient electric and magnetic fields associated with establishing a finite electrostatic dipole, Am. J. Phys. 51 (1983) 118–126.

[17] F. Napolitano, An analytical formulation of the electromagnetic field generated by lightning return strokes, IEEE Trans. Electromagn. Compat. 53 (2011) 108–113, https://doi.org/10.1109/TEMC.2010.2065810.

[18] A.K. Agrawal, H.J. Price, S.H. Gurbaxani, Transient response of multiconductor transmission lines excited by a nonuniform electromagnetic field, IEEE Trans. Electromagn. Compat EMC-22 (1980) 119–129, https://doi.org/10.1109/TEMC.1980.303824.

[19] V. Cooray, Horizontal fields generated by return strokes, Radio Sci 27 (1992) 529–537, https://doi.org/10.1029/91RS02918.

[20] M. Rubinstein, An approximate formula for the calculation of the horizontal electric field from lightning at close, intermediate, and long range, IEEE Trans. Electromagn. Compat. 38 (1996) 531–535, https://doi.org/10.1109/15.536087.

[21] M. Darveniza, A.E. Vlastos, The generalized integration method for predicting impulse volt-time characteristics for non-standard wave shapes - a theoretical basis, IEEE Trans. Electr. Insul. 23 (1988) 373–381, https://doi.org/10.1109/14.2377.

[22] A.R. Rodrigues, G.C. Guimarães, W.C. Boaventura, J.L.C. Lima, M.L.R. Chaves, A. M.B. Silva, Volt–time curve prediction of distribution insulators under standard and typical lightning overvoltages using the disruptive effect method, J. Control. Autom. Electr. Syst. 28 (2017) 259–270, https://doi.org/10.1007/s40313-016-0297-4.

[23] K. Ishimoto, F. Tossani, F. Napolitano, A. Borghetti, C.A. Nucci, Direct lightning performance of distribution lines with shield wire considering LEMP effect, IEEE Trans. Power Deliv. 37 (2022) 76–84, https://doi.org/10.1109/TPWRD.2021.3053620.

[24] A. Borghetti, K. Ishimoto, F. Napolitano, C.A. Nucci, F. Tossani, Assessment of the effects of the electromagnetic pulse on the response of overhead distribution lines to direct lightning strikes, IEEE Open Access J. Power Energy 8 (2021) 522–531, https://doi.org/10.1109/oajpe.2021.3099596.

[25] Cigré Working Group 33.01, Guide to Procedures For Estimating the Lightning Performance of Transmission Lines (TB 63), CIGRE, Paris, 1991.

[26] A. Borghetti, F. Napolitano, C.A. Nucci, F. Tossani, Influence of the return stroke current waveform on the lightning performance of distribution lines, IEEE Trans. Power Deliv. 32 (2017) 1800–1808, https://doi.org/10.1109/TPWRD.2016.2550662.

[27] A. Piantini, Lightning-induced voltages on low-voltage distribution lines, Electr. Power Syst. Res. 233 (2024), https://doi.org/10.1016/j.epsr.2024.110526.

[28] M. Nicora, D. Mestriner, M. Brignone, R. Procopio, E. Fiori, A. Piantini, F. Rachidi, Estimation of the lightning performance of overhead lines accounting for different types of strokes and multiple strike points, IEEE Trans. Electromagn. Compat. 63 (2021) 2015–2023, https://doi.org/10.1109/TEMC.2021.3060139.

[29] F. Napolitano, F. Tossani, A. Borghetti, S. Lilla, C.A. Nucci, Assessment of energy absorption by surge protective devices in low voltage lines exposed to indirect first and subsequent lightning strokes, in: 37th Int. Conf. Light. Prot, Dresden, 2024, pp. 126–131.

[30] F. Tossani, F. Napolitano, A. Borghetti, C.A. Nucci, C. Tong, Estimating flashover occurrence in distribution lines: a novel approach focused on the current-peak-to-distance ratio, Electr. Power Syst. Res. 230 (2024), https://doi.org/10.1016/j.epsr.2024.110279.

[31] V.A. Rakov, Lightning return stroke speed, J. Light. Res. 1 (2007) 80–89.

[32] F. Tossani, F. Napolitano, K. Ishimoto, A. Borghetti, C.A. Nucci, A New Calculation Method of the Lightning Electromagnetic Field Considering Variable Return Stroke Velocity, IEEE Trans. Electromagn. Compat. 63 (2021) 152–159, https://doi.org/10.1109/TEMC.2020.3015139.

[33] F. Napolitano, F. Tossani, C.A. Nucci, F. Rachidi, On the transmission-line approach for the evaluation of LEMP coupling to multiconductor lines, IEEE Trans. Power Deliv. 30 (2015) 861–869, https://doi.org/10.1109/TPWRD.2014.2318515.

[34] J.O.S. Paulino, C.F. Barbosa, I.J.S. Lopes, W.C. Boaventura, E.N. Cardoso, M. F. Guimarães, Lightning protection of overhead distribution lines installed on high resistivity soil, Electr. Power Syst. Res. 209 (2022), https://doi.org/10.1016/j.epsr.2022.107952.